SIMULATION AND MODELLING OF A SOLAR-AIDED UNDERGROUND ENERGY STORAGE SYSTEM

by

Hazel SAGLAM OZDAMAR[a], Seyit OZDAMAR[b], and Suha Orcun MERT[c*]

[a] Baskale Vocational School, Van Yuzuncu Yil University, Tusba, Van, Turkey
[b] Institute of Science, Van Yuzuncu Yil University, Tusba, Van, Turkey
[c] Department of Natural Gas and Petroleum Engineering, Iskenderun Technical University, ISTE, Iskenderun, Hatay, Turkey

Original scientific paper
https://doi.org/10.2298/TSCI220913025S

The significance of energy storage methods and related R and D studies are increasing due to the depletion of fossil fuels, rising energy prices, and growing environmental concerns. Storage of energy means elimination of practical concerns for the time difference between the time when the energy is produced and when it's needed. The importance of producing and storing energy through renewable sources is increasing every day, especially in developing countries like Turkiye, as such countries would like to reduce their dependence on foreign sources. This study focuses on an underground thermal energy storage system that was modeled for Van Region, using M-file program. The performance of an isolated day heat system as a thermal energy storage was investigated, and the thermal energy storage capacity of the system was researched for a 5 m × 5 m × 5 m soil area located on the Van Yuzuncu Yil University Campus. The temperature distribution, heat loss, and efficiency calculations were performed for a complete year and 3-D representations of the findings were obtained. The lowest efficiencies were observed in May, while the highest efficiencies were observed in July. It was found that the maximum heat loss from the system took place during December and January, and the system could be easily and effectively become a heating source for a single household with the addition of a heat pump.

Key words*: thermal energy storage, heat transfer, finite element method, underground thermal energy storage, energy efficiency*

Introduction

Today, the energy needs of the ever-increasing populations and expanding industrialization can't be met by the existing energy production facilities easily, especially for developing countries like Turkiye. In the current situation the difference between energy production and consumption is growing rapidly [1]. To meet the rapid increase in energy demand it is necessary to diversify energy production and storage methods, for which the RES are a prime candidate. Currently the majority of the world energy need is met by fossil sources such as coal, natural gas, and fuel oil. The fact that fossil fuels are depleting rapidly and there are significant environmental and economic concerns related to their use further promotes the case of renewable energy sources [2].

* Corresponding author, e-mails: orcun.mert@iste.edu.tr, orcunmert@gmail.com

Nevertheless, the constraints that are present in many of the RES like time, climate, and weather conditions makes them *unreliable* in terms of grid and energy supply security and consistency. The energy production based on these renewable *green* sources can show great variations seasonally, daily, and even between two consecutive moments. It is for this reason that a plethora of energy storage methods are being employed along with green energy production. In theory these storage methods secure grid feed and energy presence under all time and demand conditions. However, in practice these systems still need further improvements in order to perform their roles fully as intended, making research on them is important.

Energy can be stored in many different forms including biological, chemical, thermal, and electrical forms or as potential, gravitational potential, or kinetic energy [3]. In cases where the energy stored in the energy storage system (ESS) that is sustained by a RES, that particular ESS is called renewable energy storage system (RESS) [4]. The best ESS systems are considered to have the following properties: high storage capacity, high charge/discharge efficiency, low self-discharge and capacity losses, long life, cheapness, energy intensity, low weight, a high cycle number, and high charge and discharge rates.

In this study, a seasonal energy storage model was developed based on the thermal energy storage (TES) concept. Seasonal storages usually aim to store the heat in the summer and use it during the winter for heating, or they store the cold of winter to use it during the summer for cooling.

As a TES method, seasonal storage of energy in soil can be applied in different ways. The main driving force behind utilizing such soil energy usage is the fact that underground temperature is not affected by seasonal surface conditions, especially after 10-20 m ground depth range. This range is named the *Neutral Region* and presents a stable soil structure in terms of temperature. Thus, non-vertical applications for soil heat storage systems rarely go beyond 20 m depth. Vertical systems, meanwhile, use deep vertical channels borehole thermal energy storage (BTES) system, that utilize a fluid for both heating and cooling purposes, and their depth varies greatly between applications. Finally, the heat capacity of an energy-storing soil zone also changes based on its geological structure and composition [5, 6].

There are various studies in the literature regarding ESS and TESS, both from for modelling and experimental points of views, along with general overview and theory papers [7-11]. Many studies focus on modelling of heat pump systems [12, 13], and many are conducted for BTES systems [10, 11], while some of them focus on solar heat addition mechanics [7, 10, 14, 15]. There are also some economy and feasibility studies conducted for TESS and ESS systems [16-19], which are concerned with the operating and investment costs of such systems.

As an original study utilizing a novel method, the present study aims to model an underground thermal ESS in order to examine its performance metrics. The model area has a specific volume (5 m × 5 m × 5 m) that is well insulated, and stores heat obtained through solar heat systems. The study takes into consideration the temperature distribution, heat loss, and efficiency parameters, and monitors and records them for a complete year, in 3-D, for the specified volume.

Material and method

In the study, a specific soil zone located in Van Region of Turkey was used as study target area for the modelling of an underground thermal energy storage (UTES) process using the M-file program. The aim of the study was to examine the amount of heat that could be stored under the ground using a seasonal energy storage approach, challenged by the cold climate

properties of the region. The study area for TES was determined to have diameters of 5 m × 5 m × 5 m, and was deemed to be within the Van Yuzuncu Yil University Campus. In order to protect the stored thermal energy, a 25 cm thick XLPE insulation material was assumedly used as a cover around the area. This study is the modelling phase of a wider project that covers experimental studies also and the modelling is verified through the project.

The first part of the modelling was concerned with the short-time storage of the thermal energy obtained though solar water heater system. Calculations for this stage were based on the average monthly radiation amount from the Sun. The hot water was assumed to circulate in the 140 m long *U*-shaped underground pipes in the central part of the area (–2.5 m). It is here that, as the hot water circulates in the pipes, heat transfer occurs between the pipes and the soil, providing the seasonal energy storage. The physics of this second transfer and the following temperature distribution in the soil was calculated using the FEM in the M-file program.

In the study, calculations were made for two different time conditions. In the first part, the calculations were performed for the summer period when the energy was being stored into the system. The second part calculates the temperature distribution, heat loss, and efficiency calculations for the whole year, in 3-D, for the whole volume.

Modelling

For the present study, seasonal energy storage modelling for an underground thermal ESS fed through solar heat panels was performed. In the model, the hot water that transfers the solar heat to soil circulates in the underground pipes with the dimensions given in a closed cycle system.

Heat transfers from the hot water to soil in first part. The air in the soil is neglected in the calculations, and heat transfer is assumed to occur solely through conduction:

$$\Delta E_{\mathrm{st}} = E_{\mathrm{in}} - E_{\mathrm{out}} + E_{\mathrm{g}} \tag{1}$$

$$\dot{E}_{\mathrm{st}} = \frac{\mathrm{d}E_{\mathrm{st}}}{\mathrm{d}t} = \dot{E}_{\mathrm{in}} - \dot{E}_{\mathrm{out}} + \dot{E}_{\mathrm{g}} \tag{2}$$

In the model, the only energy entering the system comes through the energy transferred to the underground storage by the solar water heaters. First heat loss was neglected, but the model takes into consideration energy gains for different time periods of the year, and also the differences that occur through depth variation. The losses due to cooling are also calculated considering time and depth differences in the second part.

It is necessary to calculate the heat that will be transferred into the soil depending on time. First, the average energy from the Sun and the number of sunny days were calculated. Next, the laminar flow in the pipes and the relevant constants are calculated. The temperature distribution equation along the pipes is then evaluated. The arranged equation was coded in the M-file program by dividing the pipe into nodal points, and the temperature distribution according to the months was obtained for certain depths of the soil.

Reserve of heat energy from the oil

In seasonal energy storage area calculations, physical and thermodynamic values were assumed for a soil with a high thermal conductivity coefficient. The walls of the storage area were assumed to be covered with a thermal insulation material in order to minimize the heat losses, especially in cold months and nights. Calculations were made using an XLPE thermal insulation material with a wall thickness of 20 cm in accordance with the experimental

studies. Initial soil temperature, which is an important parameter for underground seasonal energy storage, varies depending on the region, depth, and time. From the data taken from the stations between 1970 and 2016, Baskale average (a district of Van) is $T_{\text{soilavgbaskale}} = 10.8$ °C, [20] whereas Turkey-wide average soil temperature for 100 cm depth in May is $T_{\text{soilavg}} = 15$ °C, [20]. In the model, seasonal energy storage in the study area located in Baskale town in was initiated in May, for which the initial soil temperature was [21].

A piping system similar to the horizontal ground source heat pump system was modeled to reserve the energy in the soil. Underground pipes were placed in the middle of the storage area in a *U* formation, and it is assumed that the hot water stored at day temperature circulates in closed loop underground pipes, heating the soil. Calculations were done taking into consideration the average sunshine duration and average amount of radiation for each respective month.

In the calculations the water inlet temperature is taken as $T_{\text{inw}} = 70$ °C. The outlet temperature of the water is calculated for internal and laminar flow:

$$\frac{\Delta T_{\text{o}}}{\Delta T_{\text{i}}} = \frac{T_{\text{fo}} - T_{\text{s}}}{T_{\text{fi}} - T_{\text{s}}} = \exp\left(-\frac{\rho \Delta L}{\dot{m}_{\text{w}} c_{p_{\text{w}}}} \bar{h} \right) \tag{3}$$

$$T_{\text{fo}} = \text{expexp}\left(-\frac{\rho \Delta L}{\dot{m}_{\text{w}} c_{p\,\text{w}}} \bar{h} \right)\left(T_{\text{fi}} - T_{\text{s}} \right) + T_{\text{s}} \tag{4}$$

The flow is assumed to be laminar. For constant surface temperature in laminar and fully developed conditions, the Nussellt number was accepted as 3.66 and the *h* value was calculated as 8.1×10^5 W/m^{2}K:

$$T_{\text{fo}} = 0.97\left(T_{\text{fi}} - T_{\text{s}} \right) + T_{\text{s}} \tag{5}$$

Equation 5 is used to calculate the temperature change of the fluid passing through the pipe. Having the inlet and outlet water temperatures of the underground pipes allows for the calculation of the energy released to the soil in one cycle. Heat losses due to cooling and that occur naturally on the walls were calculated during no-heating periods. Losses were calculated daily, as were the heating calculations. Net daily stored heat was obtained after heating and loss calculations for the end of each respective day, and all such calculations took into consideration the time and soil depth.

Calculation of the energy from the Sun and number of sunny days

The amount of radiation from the Sun for the Van region was taken from national meteorological database [21], and the average amount of radiation from the Sun for each month was calculated. These findings, and the average number of sunny days and sunshine durations, are displayed in tab. 1.

The total amount of heat to be added daily to the system is calculated from the eq. (6) for each of the respective months [22]:

$$Q_k = RFs\eta_k \tag{6}$$

The daily average amount of heat energy that a collector with a 30° inclination, 1.76 m^2 surface area, and 70% efficiency has been calculated, which is provided in tab. 2 for each of the respective months. The heat energy obtained was then transferred to a 300 L water system, which constitutes the preliminary storage medium.

Table 1. Solar radiation values by month [21]

Mounts	Average amount of radiation from the sun [$Wh^{-1}m^{-2}$]	Average number of sunny days per month [day]	Average daily sunshine duration [hour]
January	11.9	19.1	4.6
February	17.7	21.1	5.4
March	19.9	17.8	6.0
April	26.4	17.7	7.3
May	27.4	19.9	9.3
June	30.6	24.8	11.7
July	31.9	28	12.1
August	27.6	28.7	11.4
September	25.6	27.6	9.8
October	18.9	21.6	7.1
November	15.6	21	5.5
December	11.7	20.2	4.2

Table 2. The average daily heat energy amounts calculated for the collector according to the months

	January	February	March	April	May	June
Q_k [kWg^{-1}]	15.0	26.3	29.7	39.3	40.71	45.5
	July	August	September	October	November	December
Q_k [kWg^{-1}]	47.5	41.1	38.2	28.1	23.3	17.4

Lay-out and features of pipes and soil

Pipes were placed horizontally for decreasing the cost and ease of installation the ground. Flexible Polyethylene pipes were used as they have better resistant to corrosion and have a high heat transfer coefficient, under the ground. Underground horizontal heat exchangers are designed ¾, 1, or 1½ diameter with single-pipe horizontal heat exchangers installed at 0.5-2.5 m soil depth, and with average distance of 0.6-2.5 m. The length of pipes was taken as 140 m in order to sustain the necessary heat transfer. This size is also the upper limit that can be placed in the determined area with the given configuration as seen in fig. 1. For sake of better energy storage, the internal resistance of the pipe must be small, as it results in higher heat transfer rate and reduced energy losses. In the calculations, 1″ pipes are selected with internal resistance of $R_b = 0.159$.

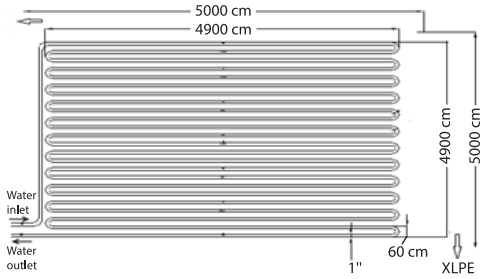

Figure 1. Lay-out of underground pipes

Soil has different thermal resistance based on its region, composition, and structure, which influences the effectiveness and efficiency of any system placed in it. The soil in Van Yuzuncu Yil University Zeve Campus is classified as clayey and is slightly moist. Soil resistivity was chosen as $R_T = 1.42$ for slightly moist and clayey soil [23].

Calculation of heat distribution with SEM method

Finite element method was used in mathematical model calculations, with varying equations for corner, inner, and edge nodes. These equations are shown in tab. 3.

Table 3. The SEM formulas of nodes by location

Position	SEM formula	
Inner node	$T_{m,n}^{p+1} = \mathrm{Fo}\left(T_{m+1,n}^{p} + T_{m-1,n}^{p} + T_{m,n+1}^{p} + T_{m,n-1}^{p}\right) + \left(1-4\mathrm{Fo}\right)T_{m,n}^{p}$	[14]
Corner node	$T_{m,n}^{p+1} = \mathrm{Fo}\left(T_{m+1,n}^{p} + 2T_{m-1,n}^{p} + T_{m,n-1}^{p}\right) + \left(1-4\mathrm{Fo}\right)T_{m,n}^{p}$	[15]
Edge node	$T_{m,n}^{p+1} = 2\mathrm{Fo}\left(T_{m+1,n}^{p} + T_{m-1,n}^{p}\right) + \left(1-4\mathrm{Fo}\right)T_{m,n}^{p}$	[16]

Since a full cycle takes place within 10 minutes according to the selected pump flow rate, the time interval steps are defined as Δt = 10 minutes. The thermodynamic properties for dry clay soil and saturated moist clay soil are listed in tab. 4.

Table 4. Soil thermodynamic properties

Soil type	Thermal conductivity [$Wm^{-1}K^{-1}$]			Constant volume heat capacity [$MJm^{-3}K^{-1}$]	Soil thermal permeability [m^2s^{-1}]		
	Minimum	Average	Maximum	Average	Minimum	Average	Maximum
Dry clay	0.4	0.5	1	1.6	0.25	0.31	0.68
Saturated moist clay	0.9	1.7	2.3	3.4	0.26	0.5	0.62

Using tab. 4, the average thermodynamic properties for the soil were calculated as 0.92 W/mK for soil thermal conductivity, 2.5 MJ/m^3 K for heat capacity, and $0.415 \cdot 10^{-6}$ m^2/s for soil thermal permeability.

It is assumed that circulation starts in underground pipes when the water stored reaches a certain temperature that is a design conditions. It was accepted that the water releases its heat and then returned to the water tank again at the defined temperature. The flow is assumed as laminar with Reynolds number of 2000. The flow rate of the water is 0.5 m^3 per hour and the power of the circulation pump was selected at 700 W. The total pipe volume has been calculated as 0.071 m^3 considering selected diameter and length. Depending on these values the cycle time is calculated as 10 minutes for water.

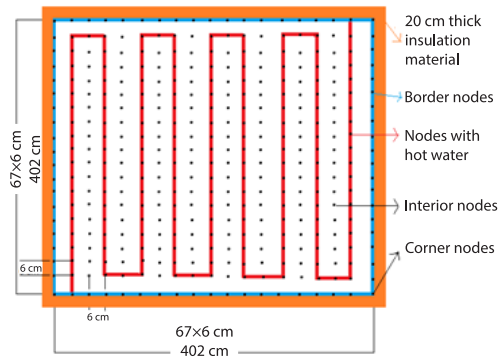

Figure 2. Lay-out representation of the 67 × 67 node on the surface section

Calculations were started by selecting the central surface in 2-D. It is assumed that the center surface has a surface area of approximately 4 m × 4 m and that there is an insulating surface of 20 cm thickness surrounding this area. Based on this, a working area where 67 × 67 nodes at 6 cm intervals covered the entire surface area with the desired sensitivity. Figure 2 shows the location of the nodes. The initial soil temperature was accepted as 10 °C in accordance with the date gathered. The total height of the system is 5 m and the distance from the center surface

to the soil surface is 2.5 m, and it is assumed that there are a total of 25 upper surface layers. Thus, the temperature and heat values in the 3-D were calculated for the whole system. The main result is the temperature for all surfaces. The amount of heat lost by all surface nodes and their sums that is emerged as the total amount of heat lost in the system calculated based on the temperature of the boundary nodes and the surface areas calculated in the direction of the height and spacing of the boundary nodes, and the insulation temperature difference calculated depending on the boundary node and soil temperature.

Results and discussion

For the design in which the seasonal ESS is applied, the calculations and temperature distributions are shown as 3-D diagrams, using the M-file program. In the modelling, the temperature distribution graphs for the center (–2.5 m) and the upper surface (0 m) of the storage area according to the months were created for two different situations. The results of the calculations for the center (–2.5 m) surface temperatures before and after heat loss are shown in fig. 3 for each month separately.

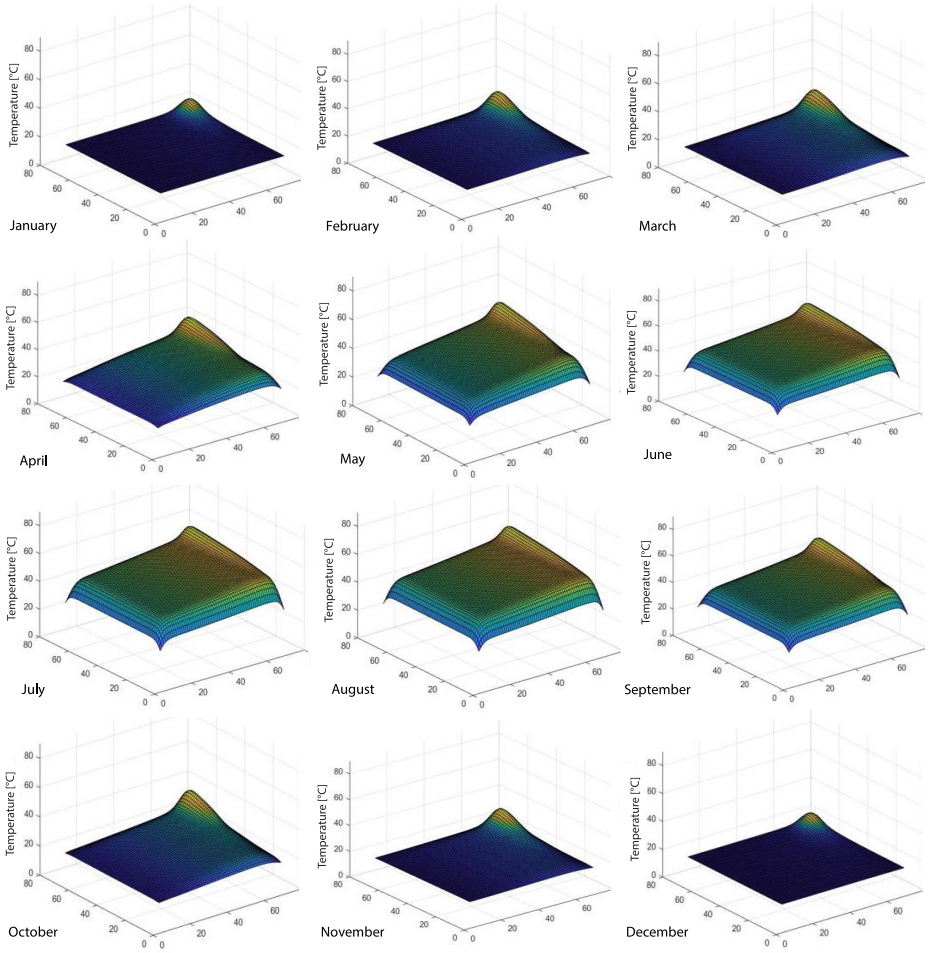

Figure 3. Temperature distributions at the center surface (–2.5 m) including the heat losses of the seasonal energy storage area

According to the results, it is understood that the downward concave temperature drop on the center surface in the *x*-direction is the general behavior. In the *Y*-direction, linear temperature drops were observed compared to the previous node group. After losing heat, it behaves in a softer slope compared to the situation before heat loss. The main reason for this is that the maximum temperature points get closer to the average values due to more heat loss than the average values.

Nodes with average and below average temperature values, on the other hand, have less tendency to display changes in their temperature values, since less heat loss occurs in them. During the months in which the heat is withdrawn from the system (October-November-December-January-February-March-April), a sudden decrease in temperature can be observed. The reason for this the reduced amount of heat entering the system, especially in the cold months, as the radiation from the Sun is reduced. Accordingly, the small amount of solar heat entering the system is rapidly lost, resulting in a temperature drop.

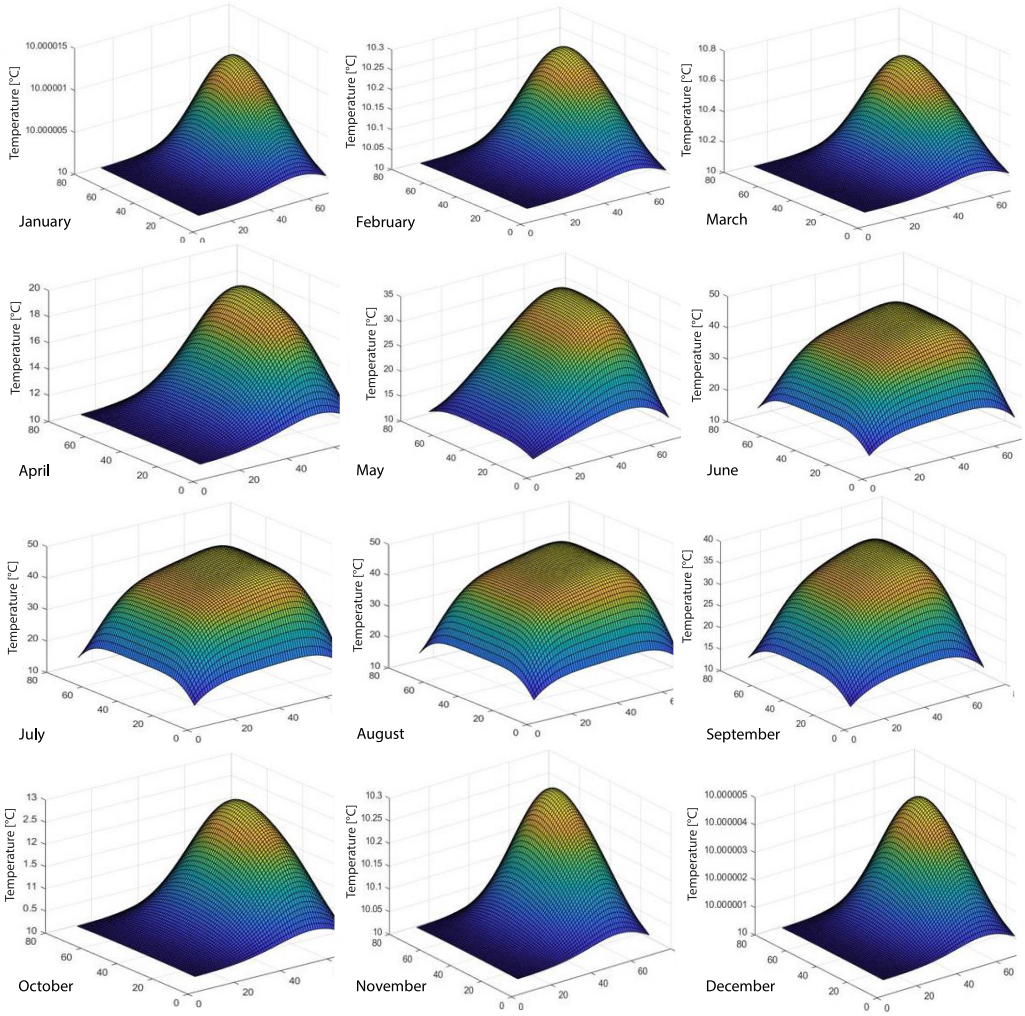

Figure 4. Temperature distributions on the upper surface (0 m) including the heat losses of the seasonal energy storage area

The maximum temperature average values during the year were spotted in July and the minimum temperature average values were occurred in December. When the data were examined, it was seen that the highest yield and temperature values took place in July, and the lowest yield and temperature values were obtained in December.

The temperature distribution calculations according to the months after the heat loss for the layer on the top surface are shown in fig. 4. It is observed that the temperature is high in certain regions, especially in cold months. Since the temperature difference between the soil and the hot water is high in the part where the hot water inlet is located, the heat transfer at this location is rapid. As a result, the hot water loses most of its heat initially, due to which less temperature increase is observed in other parts.

Due to the low amount of radiation from the sun in cold months, there is not enough heat input to the system. When the hot months are examined, it is observed that the temperature distribution is more homogeneous due to the increase in the amount of heat entering the soil. The reason for this is that the heat transfer is slower due to the heating of the hot water inlet over time, and the hot water can transfer heat along the pipe. Here, the highest temperature is in July and the lowest temperature is in December.

In the study, the losses against the heat given to the system daily to the storage area were also calculated. Based on these values, the thermal efficiency of the system is calculated. The comparison of heat loss and efficiency values by months was made according to the data on the last day of the month and the results are shown in figs. 5 and 6.

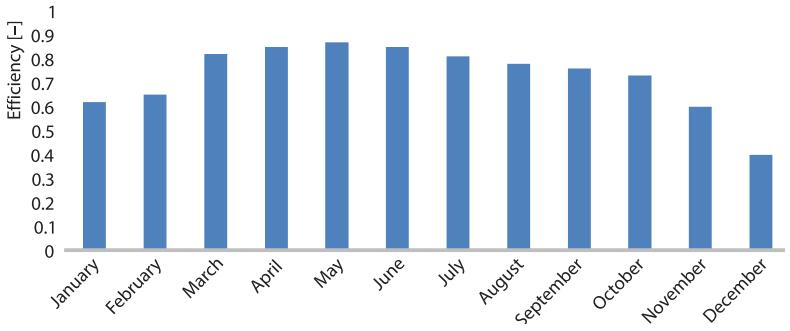

Figure 5. Efficiency values for the last day of the month in storage

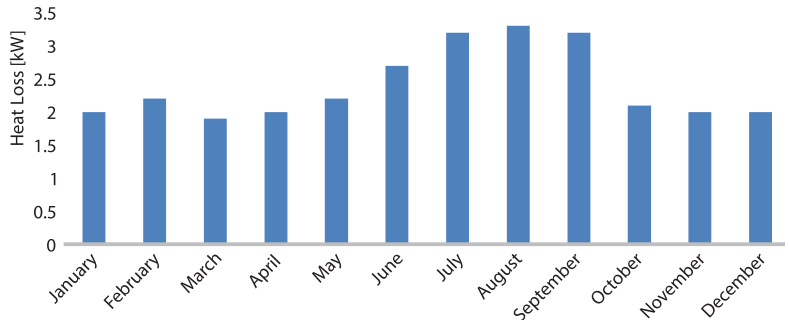

Figure 6. Heat loss values for the last day of each month in the storage area

When the heat loss and yield graphs are examined, the yield values decrease linearly day by day with the saturation of the soil with heat in general. The most important factor in the decrease in efficiency and increase in heat loss is the increase in heat loss with the increase in

the temperature of the wall nodes. At the same time, the heat shrinkage of a mass with increasing temperature decreases depending on time.

In the winter months, the lowest values of the yield for the year are observed. The reason for this is the low amount of radiation coming from the Sun in the winter months, and the increased heat loss due to environmental conditions. As can be seen, heat losses increase linearly as the days progress. The highest yields were observed in the summer months as expected. The reasons for this are the increase in the amount of radiation coming from the Sun in conjunction with the decrease in heat losses due to increased soil temperature.

Conclusions

In this study, the mathematical modelling of a systems which was conducted for the purpose of examining a solar-assisted seasonal underground ESS was performed using an in-house developed M-file routine. While creating the mathematical model, the thermal distribution was considered to occur not only as in a flat plate, but in a zigzag shape taking into consideration the depth of the soil. This approach provided a model that was close to reality in terms of feasibility.

In addition, the model was created by assuming that the cooling occurs simultaneously at all sides of the system and the differences in the conditions based on time -like soil heat and average solar radiation- were also considered. This approach helped to achieve realistic and accurate results.

The system not only takes into consideration the warming up and cooling down at the time of solar energy input, but also during the cooling phase that occurs at the end of the sunbathing period. In addition all these, the model was divided into layers in terms of depth, considering that it would allow the examination in the 3-D, and temperature distribution calculations were performed for each of the corresponding layers.

In the study model, seasonal energy storage was initiated in May, based on the solar radiation values obtained from national meteorological databases. Initially, a rapid warming occurred in the model due to the low temperature of the storage area soil. As the temperature of the storage area increased over time, the heat transfer slowed down. This shows the expected phenomena of the soil reaching saturation with thermal energy with decreasing temperature difference between the soil and heated water after a certain temperature value.

It was determined that, at certain period of the simulated year, the temperature of the storage area decreased due to the cooling of the air, and the decrease in the amount of solar radiation. The highest temperature for the storage area was calculated value for July, while the coldest temperature value was determined for December. According to the results of the study, it has been deduced that if a heat pump is added to the system, it can be used as a potential a heating source for a single house. It is estimated that addition of a heat pump to create a hybrid system will increase the COP value and decrease the household electricity consumption.

Acknowledgment

This work has been supported by Van Yuzuncu Yil University Scientific Research Projects Coordination Unit under Grant No. FBA-2019-7774.

Nomenclature

c_{p_w} – specific heat of water, [kWhkg^{-1}K^{-1}]
E_g – heat generation
E_{in} – total energy entering the system
E_{out} – total energy entering the system
ΔE_{st} – change in the total energy of the system
$\dot{E}_g$ – rate of net energy transfer in by heat generation
$\dot{E}_{in}$ – rate of net energy transfer in by heat, work, and mass

$\dot{E}_{out}$ – rate of net energy transfer out by heat, work, and mass
$\dot{E}_{st}$ – rate of change in internal kinetic, potential, *etc*., energies
F – correction factor for collector mounting tilt angle, [–]
Fo – Fourier number
$\overline{h}$ – average heat transfer coefficients, [$Wm^{-2}K^{-1}$]
$T_{soilavgbaskale}$ – soil average temperature at 100 m depth for Baskale region
$T_{soilavg}$ – soil average temperature at 100 m depth for Turkey
T_{inw} – inlet water temperature
T_i – initial temperature of the water in the tank, [°C]
T_o – final temperature of the water in the tank, [°C]
T_{fo} – outlet water temperature, [°C]
T_{fi} – inlet water temperature, [°C]
T_s – surface temperature, [°C]
ΔL – between distance of nodes
m – notation by position in the x-direction
$\dot{m}_w$ – volume flow rate of water, [m per hour]
p – notation by time
n – notation by position in the y direction
Q_k – value of energy collected in the collectors, [kW]
R – value of radiation from the Sun, [Wm^{-1}]
R_b – pipes resistance
R_T – soil resistance
s – collector area, [m^2]
Δt – time distance

Greek symbols

η_k – efficiency of collector
ρ – water density

Acronyms

BTES – borehole thermal energy storge
ESS – energy storage system
RESS – renewable energy storge system
TES – thermal energy storage
UTES – underground thermal energy storage
XLPE – cross-linked polyethylene

References

[1] Yakut, R., *et al*., Experimental and Numerical Investigations of Impingement Air Jet for a Heat Sink, *Procedia Engineering*, *157* (2016), Dec., pp. 3-12
[2] Hadjipaschalis, I., *et al*., Overview of Current and Future Energy Storage Technologies for Electric Power Applications, *Renewable and Sustainable Energy Reviews*, *13* (2009), 6-7, pp. 1513-1522
[3] Boztepe, M., Enerji Depolama. Retrieved from http://electronics.ege.edu.tr/boztepe/cgibin/%0Aload.cgi?gee591_lecture6.pdf,%0A, 2012
[4] Kozak, M., Kozak, S., ENERJİ DepolamaYöntemleri, Süleyman Demirel Üniversitesi Uluslarası Teknolojik (in Turkish), *Bilimler Dergisi*, *4* (2012), 2, pp. 17-29
[5] Yilmazoglu, M. Z., Isı Enerjisi Depolama Yöntemleri ve Binalarda Uygulanması (Heat Energy Storage Methods and Application in Buildings – in Turkish), *Politeknik Dergisi*, *13* (2010), 1, pp. 33-42
[6] Dikici, D., Doğal Soğuk Kaynaklardan Yararlanan Yer Altı Kanallarında Termal Enerji Depolanması, In Çukurova Üniversitesi Fen Bilimleri Enstitüsü Kimya Anabilim Dalı (Thermal Energy Storage in Six Channels – in Turkish), Adana, Turkey, 2004
[7] Alva, G., *et al*., Thermal Energy Storage Materials and Systems for Solar Energy Applications, *In Renewable and Sustainable Energy Reviews*, *68* (2017), Part 1, pp. 693-706
[8] Kocak, B., *et al*., Review on Sensible Thermal Energy Storage for Industrial Solar Applications and Sustainability Aspects, *In Solar Energy*, *209* (2020), Oct., pp. 135-169
[9] Sarbu, I., Sebarchievici, C., A Comprehensive Review of Thermal Energy Storage, *In Sustainability*, *10* (2018), 1
[10] Suresh, C.,Saini, R. P., Review on Solar Thermal Energy Storage Technologies and Their Geometrical Configurations, *In International Journal of Energy Research*, *44* (2020), 6
[11] Yang, T., *et al*., Seasonal Thermal Energy Storage: A Techno-Economic Literature Review, *In Renewable and Sustainable Energy Reviews*, *139* (2021), Apr., 110732
[12] Hasan, I. H., Yumrutas, R.. Investigation of a Solar Assist*ed Heat Pump Heat Drying System with Underground Thermal Energy Storage Tank, Solar Energy,* 199 (2020), Feb., pp. 538-551
[13] Inalli, M., Design Parameters for A Solar Heating System with an Underground Cylindrical Tank, *Energy*, *23* (1998), 12, pp. 1015-1027
[14] Oosterbaan, H., et al., Numerical Thermal Back-calculation of the Kerava Solar Village Underground Thermal Energy Storage, *Procedia Engineering*, *191* (2017), Dec., pp. 352-360
[15] Tordrup, K. W., *et al*., An Improved Method for Upscaling Borehole Thermal Energy Storage Using Inverse Finite Element Modelling, *Renewable Energy*, *105* (2017), May, pp. 13-21
[16] Abokersh, M. H., *et a*l., A Framework for Sustainable Evaluation of Thermal Energy Storage in Circular Economy, *Renewable Energy*, *175* (2021), Sept., pp. 686-701

[17] Esen, H., *et al.*, A Techno-Economic Comparison of Ground-Coupled and Air-Coupled Heat Pump System For Space Cooling, *Building and Environment*, *42* (2007), 5, pp. 1955-1965
[18] Nhut, L. M., *et al*., A Parametric Study of a Solar-Assisted House Heating System with A Seasonal Underground Thermal Energy Storage Tank, *Sustainability*, (Switzerland), *12* (2020), 20
[19] Chung, M., *et al*., Simulation of a Central Solar Heating system with Seasonal Storage in Korea, *Solar Energy*, *64* (1998), 4-6, pp. 163-178
[20] ***, Anon-im. (n.d.-c). Ölçülen En Düşük Toprak Sıcaklıkları - Meteoroloji Genel Müdürlüğü.
[21] ***, Anon-im. (n.d.-b). İllere göre Radyasyon Değerleri - Meteoroloji Genel Müdürlüğü.
[22] ***, Anon-im. (n.d.-a). Güneş Enerjisi Kollektör Hesabı ve Tesisat Bağlantıları | Tesisat.
[23] Miles, L., Heat Pump Theory and Services, in: *The HVAR Training Authority*, Delmar Publishers Inc. Huntington Beach, Cal., USA, 1994

Paper submitted: September 13, 2022
Paper revised: October 29, 2022
Paper accepted: November 6, 2022